32nd European Modeling & Simulation Symposium
17th International Multidisciplinary Modeling & Simulation Multiconference

ISSN 2724-0029 ISBN 978-88-85741-44-7 © 2020 The Authors.
DOI: 10.46354/i3m.2020.emss.031

Modeling and Implementation of An ADC based Grid-Connected Voltage Source Inverter for Real-Time Simulation Based on FPGA

Chunyu Zhang[1,2,*], Shouxiang Wang[1,2] , Yanan Zhou[3] and Guoqiang Zu[4]

[1] Key Laboratory of Smart Grid of Ministry of Education, Tianjin University, Tianjin 300072, China
[2] Tianjin Key Laboratory of Power System Simulation and Control, Tianjin University, Tianjin 300072, China
[3] Tianjin Electric Power Company, Tianjin 300072, China
[4] Tianjin Electric Power Research Institute, Tianjin 300072, China

[*] Corresponding author. Email address: chunyu8088@tju.edu.cn

Abstract

With the development of distributed generations, the related real-time simulation technology has drawn extensive attention. In the distributed generation units, the power electronics are critical parts. In order to better deal with challenges of the large number of power electronic devices connected to the distribution network, this paper presents an embedded real-time simulation model based on associated discrete circuit (ADC) for a three-phase voltage source inverter. This model can be implemented in a field-programmable gate array (FPGA). And the FPGA can reduce the computational burden of power electronics simulation, because of its powerful parallel computing performance. First of all, a grid-connected power electronic inverter with a three phase RL filter model is built based on the ADC modeling approach, which can enhance the small step simulation performance. Secondly, the phase-locked loop technology has been introduced into the system to track the information of the phase angle. Finally, a FPGA based voltage and current double loop control method is presented to ensure the stable operation. The circuit simulation results verify the effectiveness of the scheme.

Keywords: Distributed generation units, Voltage source inverter (VSI), Real-time simulation, Associated discrete circuit (ADC), Field-programmable gate array (FPGA), Hardware-in-loop (HIL)

1. Introduction

Nowadays, Hardware in the loop (HIL) real-time simulation has been widely applied in in many engineering fields to reduce operation costs. The development power electronic technology promotes the development of distributed generation units and modern smart grid technology. As power electronics technology matures, power electronics devices will be widely connected to the grid to improve its flexibility. Meanwhile, HIL real-time simulation of power electronics devices on field-programmable gate array (FPGA) has gained more attractiveness (Mu et al., 2014; Guo et al., 2018). So far, the commercial off-line power system electromagnetic simulation programs include EMTP-RV, ATP-EMTP, PSCAD-EMTDC, etc. Compared with them, FPGA has powerful parallel computing performance, which can ensure the simulation system run in nature time to meet the challenges of small step simulation and fast calculation (Dagbagi et al., 2016).

There are two commonly used methods to simulate the behavior of the high frequency switching device

© 2020 The Authors. This article is an open access article distributed under the terms and conditions of the Creative Commons Attribution (CC BY-NC-ND) license (https://creativecommons.org/licenses/by-nc-nd/4.0/).

(Hadizadeh et al., 2019; Huang and Dinavahi, 2019): 1) the piecewise linear approach, which divides the switching state into two working sections. The switch is modeled as a very small resistance when the switch state is ON, and large when the switch state is OFF. 2) associate discrete circuit (ADC), which represents the switching state into an inductor and a capacitor in series with a resistor when switch is ON and OFF, respectively. ADC method integrates the current flow at t-Δt as a current source in the circuit to calculate the current flow at t, and the equivalent modes of the ON and OFF state of the switch are shown in Fig.1. The first approach needs to solve a system of equations with varying node admittance matrix, which caused by the change of parameters. As a result, this method requires heavier computations. In the second ADC method, the parameters of the circuit can be chosen to keep constant the extracted conductance matrix whatever the state of the power switches (Matar and Iravani, 2010). In this way, the computational complexity can be greatly reduced.

Dagbagi et al. (2016) presents a converter model for real-time simulation based on ADC method, but the real-time measurement of phase angles of the grid is neglected. Hadizadeh et al. (2018) describes an online matrix-inversion technique based on Sherman–Morrison–Woodbury formulas. Liu et al. (2018) describes a hybrid modeling approach for real-time simulation of power electronic devices. However, in the process of simulation, the inverse function block needs to be called at each step to solve the inverse of the node admittance matrix in Hadizadeh et al. (2018) and Liu et al. (2018). Therefore, the further reduction of simulation step size is limited. a FPGA-based real-time digital simulator for a realistic power electronic apparatus is presented in Myaing and Dinavahi (2010). But its versatility is limited by the diversity of power electronic equipment in practice. An off-grid DC-DC converter with non-isolated coupled inductor in solar system is presented in Umadevi and Nagarajan (2019), which neglects the behavior of the grid. And FPGA is mainly used to complete the control loop of the system, which provides an idea for the further development of FPGA.

Moreover, digital controllers also can be embedded into the FPGA to ensure the operation of the system, such as model predictive control (Bayhan, Abu-Rub and Balog, 2016), deadbeat control (Daisuke et al., 2006), PI control (Harahap, 2015; Juarez-Abad et al., 2014), etc. The computing time of the controller can be greatly reduced by using FPGA. In addition, the functions such as observation, estimation, or diagnostic can be ensured.

Nomenclature

FPGA	Field-programmable gate array
HIL	Hardware-in-loop
VSI	Voltage source inverter
DGUs	Distributed generation units
PLL	Phase-locked loop
Θ	Phase angle
C_s	Equivalent capacitance of the switch model
L_s	Equivalent inductance of the switch model
R_s	Equivalent resistance of the switch model
Δt	Sample interval
V_{dc}	DC side voltage
V_{La}	AC side A phase output voltage of inverter
V_{Lb}	AC side B phase output voltage of inverter
V_{Lc}	AC side C phase output voltage of inverter
i_{La}	A phase current of inverter
i_{Lb}	B phase current of inverter
i_{Lc}	C phase current of inverter
L_a	A phase inductance
L_b	B phase inductance
L_c	C phase inductance
R_{La}	A phase current
R_{Lb}	B phase current
R_{Lc}	C phase current
J_S	Historical current value of the switch
J_D	Historical current value of the diode

In this paper, a real time simulation on FPGA method of grid-connected PWM inverter based on ADC is proposed. Besides, a voltage current double closed loop digital controller is also embedded into the real time simulation system. In order to capture line phase angle information, the phase-locked loop (PLL) technique as the state-of-the-art method introduced into the real time simulation system.

The remainder of this paper is organized as follows. The power electronic inverter real time simulation model is presented in section 2. Section 3 gives the implementation of the voltage source inverter model. Section 4 concludes this paper.

2. Power electronic inverter real time simulation model based on FPGA

In this section, the digital time-domain simulation model of a grid-connected power electronic inverter unit based on ADC method is carried out. Moreover, different real-time models of other elements are also built to support the operation of the system.

2.1. ADC based switch model

As shown in Figure 1, different behaviors of the switch can be represented by different component. And the difference equation of different states of the switch using trapezoidal difference method can be represented as:

$$\begin{cases} i_{\mathrm{ON}}(t) = \dfrac{\Delta t}{2L_s}u(t) + A_{1\mathrm{ON}}u(t-\Delta t) + A_{2\mathrm{ON}}i(t-\Delta t) \\ i_{\mathrm{OFF}}(t) = \dfrac{2C_s}{2C_sR_s+\Delta t}u(t) - A_{1\mathrm{OFF}}u(t-\Delta t) \\ +A_{2\mathrm{OFF}}i(t-\Delta t) \end{cases} \quad (1)$$

where $A_{1\mathrm{ON}} = \frac{\Delta t}{2L_s}$, $A_{2\mathrm{ON}}=1$,$A_{1\mathrm{OFF}} = \frac{2C_s}{2C_sR_s+\Delta t}$, $A_{2\mathrm{OFF}} = \frac{2C_sR_s-\Delta t}{2C_sR_s+\Delta t}$, and Δt is the sampling interval.

In order to keep the extracted conductance matrix constant during different states of the power switches, the value of the parameters can be chosen as:

$$\frac{\Delta t}{2L_s} = \frac{2C_s}{2C_sR_s+\Delta t} \quad (2)$$

After setting the appropriate parameters, the computational burden associated with the admittance matrix inversion can be avoided to enhance the computational efficiency of the solver.

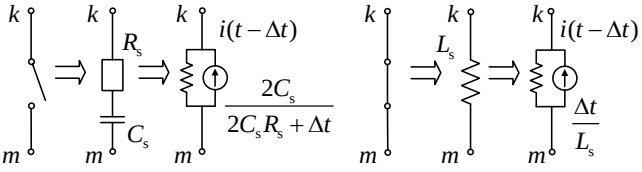

Figure 1 Switch and ADC equivalent switch model

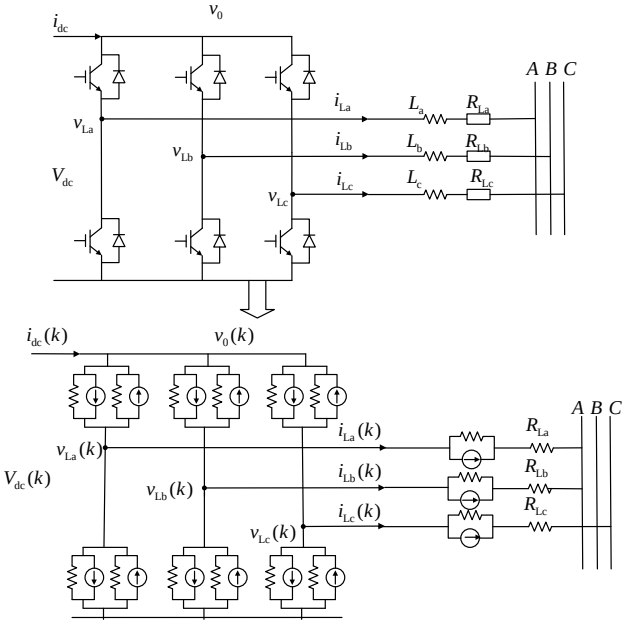

Figure 2 Example application: Power electronic inverter and the corresponding discretized model

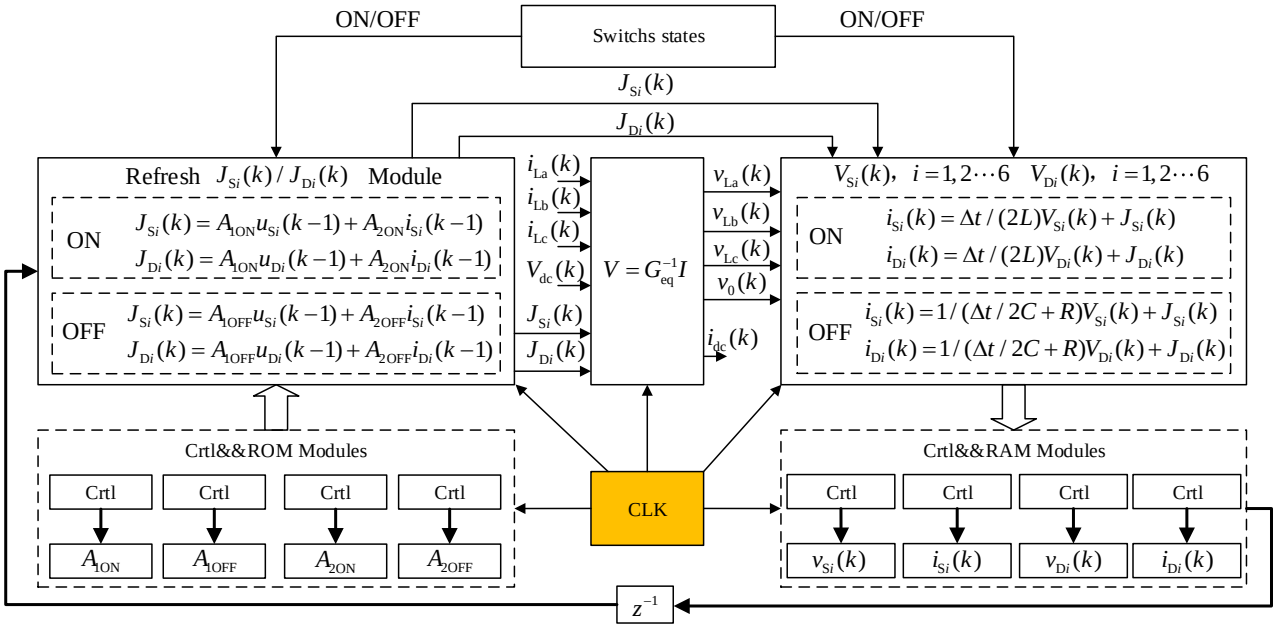

Figure 3. Calculation flow diagram of the ADC-based model

2.2. Power electronic inverter unit model

The ADC based real time simulation model of a three-phase two-level power electronic inverter unit is shown in Figure 2. A nodal analysis is made to extract the relations between voltages and currents of the whole power inverter. The relations can be mathematically represented by:

$$G_{\mathrm{eq}}V[k] = I[k] \tag{3}$$

Where $G_{\mathrm{eq}}$is the node admittance matrix, $V[k]$ represents the voltage of node k and $I[k]$ is the current of branch k. For the three phase two level power electronic inverter, where the expressions of them are:

$$G_{\mathrm{eq}} = \begin{bmatrix} 3(G_S+G_D) & -(G_S+G_D) & -(G_S+G_D) & -(G_S+G_D) & -1 \\ -(G_S+G_D) & 2(G_S+G_D) & 0 & 0 & 0 \\ -(G_S+G_D) & 0 & 2(G_S+G_D) & 0 & 0 \\ -(G_S+G_D) & 0 & 0 & 2(G_S+G_D) & 0 \\ 1 & 0 & 0 & 0 & 0 \end{bmatrix}$$

$$V[k] = [v_0(k) \quad v_{\mathrm{La}}(k) \quad v_{\mathrm{Lb}}(k) \quad v_{\mathrm{Lc}}(k) \quad i_{\mathrm{dc}}(k)]^T$$

$$I[k] = \begin{bmatrix} J_{\mathrm{D1}}(k) - J_{\mathrm{S1}}(k) + J_{\mathrm{D3}}(k) - J_{\mathrm{S5}}(k) + J_{\mathrm{D5}}(k) - J_{\mathrm{S5}}(k) \\ J_{\mathrm{S1}}(k) - J_{\mathrm{D1}}(k) + J_{\mathrm{D4}}(k) - J_{\mathrm{S4}}(k) - i_{\mathrm{La}}(k) \\ J_{\mathrm{S3}}(k) - J_{\mathrm{D3}}(k) + J_{\mathrm{D6}}(k) - J_{\mathrm{S6}}(k) - i_{\mathrm{Lb}}(k) \\ J_{\mathrm{S5}}(k) - J_{\mathrm{D5}}(k) + J_{\mathrm{D2}}(k) - J_{\mathrm{S2}}(k) - i_{\mathrm{Lc}}(k) \\ V_{\mathrm{dc}}(k) \end{bmatrix}$$

Where G_s and $G_D$are the corresponding admittance of switches and diodes, J_s and $J_D$represent the equivalent historical current sources. As a consequence, the nodal voltages can be calculated as:

$$V[k] = G_{eq}^{-1}I[k] \tag{4}$$

The calculation flow diagram of the ADC-based model is shown in Figure 3. As shown in Figure 3, the current instant nodal voltages are used to calculate the current values at this instant, and they are stored into the on-chip ROMs as the historical current values, and the calculation flow is represented in Figure 4. Moreover, in order to reduce the computational burden, the corresponding $A_{1\mathrm{ON}}$, $A_{2\mathrm{ON}}$ $A_{1\mathrm{OFF}}$ $A_{2\mathrm{OFF}}$ are precomputed by principal computer and stored into the On-chip RAMs.

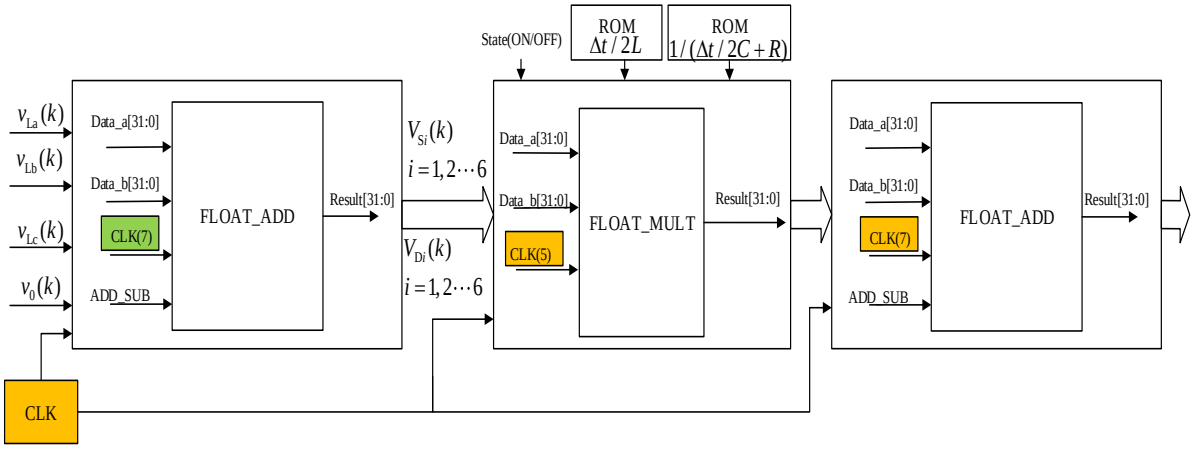

Figure 4. Calculation flow diagram of the current

2.3. Three-phase RL filter model

As shown in Figure 2, after a backward Euler approximation, the discrete-time current equations of the three-phase RL filter can be calculated as (Dagbagi et al., 2016):

$$\begin{aligned} i_{\mathrm{La}}(k) &= a_1[v_{\mathrm{La}}(k) - v_{\mathrm{ga}}(k)] + a_2 i_{\mathrm{La}}(k-1) \\ i_{\mathrm{Lb}}(k) &= a_1[v_{\mathrm{Lb}}(k) - v_{\mathrm{gb}}(k)] + a_2 i_{\mathrm{Lb}}(k-1) \\ i_{\mathrm{Lc}}(k) &= a_1[(v_{\mathrm{Lc}}(k) - v_{\mathrm{gc}}(k)] + a_2 i_{\mathrm{Lc}}(k-1) \end{aligned} \tag{5}$$

where $a_1 = \frac{\Delta t}{R\Delta t + L}$, $a_2 = \frac{L}{R\Delta t + L}$, which also can be prestored into the on-chip ROMs for reading and calculation.

2.4. PLL model

The PLL technique is one of the state-of-the-art methodes to extract the phase angle of the grid voltages (Blaabjerg, et al., 2006 and Blaabjerg, Chen and Kjaer, 2004), which is a basic information for grid-connected power conditioning devices.

The PLL circuit consists of three components: phase detector (PD), loop filter (LPF) and voltage-controlled oscillator (VCO). The structure of PLL is presented in Figure 5.

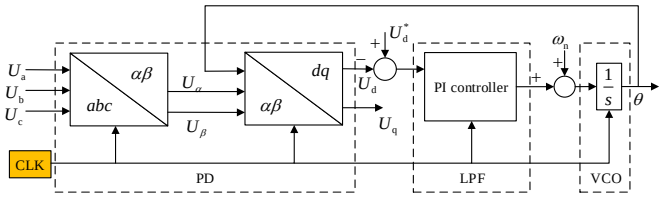

Figure 5 Structure of PLL

As shown in Figure 5, the coordinate transformation forms $abc \rightarrow \alpha\beta \rightarrow dq$ are needed for the realization of PLL. The output of PLL is the phase angle, which will be fed back to the $\alpha\beta \rightarrow dq$module of PD to compute U_d. The error between the measured U_d and U_d^* is regulated by the PI controller, and its output is the grid frequency. And the information of phase angle can be obtained by integration with respect to the grid frequency.

2.5. PI controller model

There are many control elements to guarantee the stable operation of the devices, and the most commonly used for power electronics devices is PI control. The general expression of PI controller transfer function is:

$$u(s) = (K_p + \frac{K_i}{s})x(s) \qquad (6)$$

where K_p and K_i are the coefficients of proportional control and integral control, respectively. In order to embed the digital controller in the FPGA, the PI control transfer function should be discretized by difference equations. After a trapezoidal difference approximation, the corresponding discrete-time equations are expressed as:

$$u(t) = A_1 x(t) + A_2 x(t - \Delta t) + A_3 u(t - \Delta t) \qquad (7)$$

where $A_1 = \frac{\Delta t}{2} K_i + K_p$, $A_2 = \frac{\Delta t}{2} K_i - K_p$, $A_3 = 1$. As a result, the structure of PI controller module can be presented as in Figure 6.

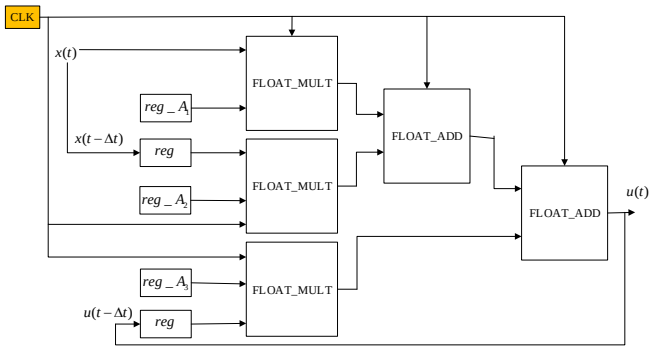

Figure 6 Structure of PI controller

3. Implementation of the voltage source

inverter model

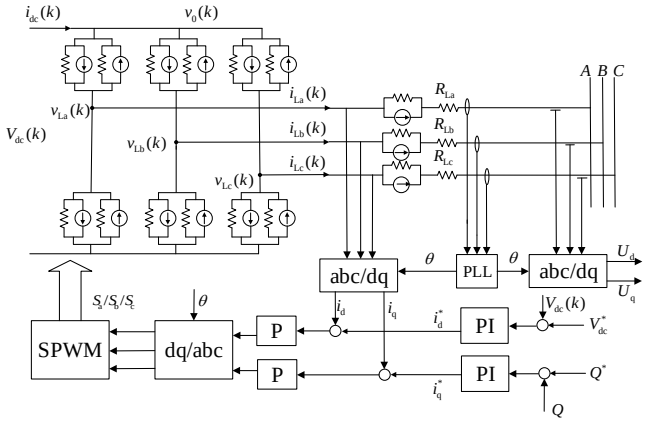

Figure. 7 Structure of the overall system

The overall system is shown in Figure 7. The values of PI controller coefficients are: $K_p = 2.85$, $K_i = 1268.35$, $V_{\mathrm{dc}} = 380V$, $\omega_n = 628\mathrm{rad/s}$ and the sample interval is 10us(with a 50-MHz system clock). The outputs of the sinusoidal pulse width modulation (SPWM) signal and the three-phase output voltages are presented in Figure 8 and Figure 9, respectively. They are both obtained on the platform of *Modelsim 10.7* software. The inverter model is built on the chip of Altera Stratix V 5SGXEB6R1F43C2. As presented in Figure 8, three pairs of complementary pulse signals are generated by the SPWM element to drive the actions of switches. Moreover, as shown in Figure 9, the three-phase output voltages have the same amplitude (250V) and the phase difference is 2π/3. The results show that the output voltages of the system can track the grid voltage.

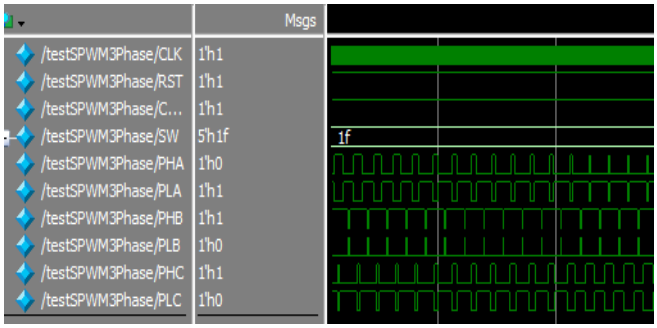

Figure 8. Three phase complementary PWM signal

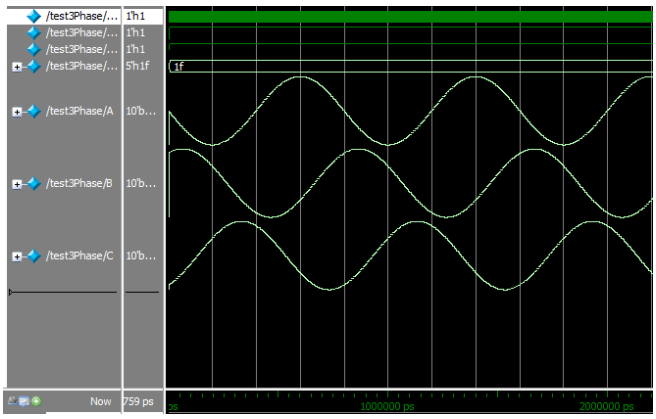

Figure 9. Three phase voltage of the inverter

4. Conclusion

In this paper, an embedded real-time simulation approach has been presented for a three-phase voltage source inverter with a three phase RL filter based on ADC modeling approach. The real time simulator can be implemented in a FPGA. The FPGA can reduce the computational burden of power electronics simulation, because of its powerful parallel computing performance. In order to track the voltage phase angle, a PLL technology is also introduced into the system. Finally, A FPGA based voltage and current double loop digital controller is presented for the simulation system to ensure the service continuity. Effectiveness and accuracy of the proposed scheme has been verified by circuit simulation.

Acknowledgment

This work is supported by the State Grid Corporation of China Science and Technology Project (No.SGTJDK00PJJS2000072).

References

Mu, Q. , Liang, J. , Zhou, X. , Li, Y. and Zhang, X. . (2014). Improved ADC model of voltage-source converters in DC grids. *IEEE transactions on power electronics*, 29(11): 5738-5748.

Guo, X. , Yuan, J. , Tang, Y. and You, X. . (2018). Hardware in the loop real-time simulation for the associated discrete circuit modeling optimization method of power converters. *Energies*, 11(11).

Dagbagi M. , Hemdani A. , Idkhajine L. , Naouar M. W. , Monmasson E. and Slama-Belkhodja I. . (2016). ADC-based embedded real-time simulator of a power converter implemented in a low-cost FPGA: application to a fault-tolerant control of a grid-connected voltage-source rectifier. *IEEE transactions on industrial electronics*, 63(2): 1179-1190.

Hadizadeh, A. , Hashemi, M. , Labbaf, M. and Parniani, M. . (2018). A matrix-inversion technique for FPGA-based real-time EMT simulation of power converters. *IEEE transactions on industrial electronics*, 66(2): 1224-1234.

Myaing, A. , and Dinavahi, V. . (2010). FPGA-based real-time emulation of power electronic systems with detailed representation of device characteristics. IEEE Transactions on Industrial Electronics, 58(1), 358-368.

Umadevi K. and Nagarajan C. . (2019). Design and implementation of novel soft switching method based DC-DC converter with non-isolated coupled inductor in solar system using FPGA. *Microprocessors and Microsystems.* 73(2020): 1.

Huang, Z. , and Dinavahi, V. . (2019). A fast and stable method for modeling generalized nonlinearities in power electronic circuit simulation and its real-time implementation. *IEEE transactions on power electronics*, 34(4): 3124-3138.

Matar M. and Iravani R. . (2010). FPGA implementation of the power electronic converter model for real-time simulation of electromagnetic transients. *IEEE transactions on power delivery*, 25(2): 852-860.

Liu, C. , Ma, R. , Bai, H. , Li, Z. , Gechter, F. and Gao, F. . (2018). Hybrid modeling of power electronic system for hardware-in-the-loop application. *Electric Power Systems Research*, 163(OCT.), 502-512.

Bayhan, S. , Abu-Rub, H. and Balog, R. S. . (2016). Model predictive control of quasi-z-source four-leg inverter. *IEEE transactions on industrial electronics*, 63(7): 4506-4516.

Daisuke, Y. , Kawakami, N. , Ota, S. and Yokoyama, T. . (2006 June 18-22). Comparison of FPGA based digital control method for low carrier-frequency PWM inverter. *37th IEEE power electronics specialists conference.*

Harahap, C. R. . (2015). FRIT based PI tuning for speed control of PMSM using FPGA for high frequency SiC MOSFET inverter. ICIEV. *IEEE.*

Juarez-Abad, J. , Linares-Flores, J. , Guzman-Ramirez, E. and Sira-Ramirez, H. . (2014). Generalized proportional integral tracking controller for a single-phase multilevel cascade inverter: an fpga implementation. *IEEE transactions on industrial informatics*, 10(1): 256-266.

Blaabjerg, F. , Teodorescu, R. , Liserre, M. and Timbus, A. V. . (2006). Overview of control and grid synchronization for distributed power generation systems. *IEEE transactions on industrial electronics*, 53(5): 1398-1409.

Blaabjerg, F. , Chen, Z. and Kjaer, S. B. . (2004). Power electronics as efficient interface in dispersed power generation systems. IEEE transactions on power electronics, 19(5): 1184-1194.